

Ground-state phases of the spin-1/2 J_1 - J_2 Heisenberg antiferromagnet on the square lattice: A high-order coupled cluster treatment

R. Darradi¹, O. Derzhko^{1,2}, R. Zinke¹, J. Schulenburg³, S. E. Krüger⁴, and J. Richter¹

¹*Institut für Theoretische Physik, Universität Magdeburg, P.O. Box 4120, 39016 Magdeburg, Germany*

²*Institute for Condensed Matter Physics, National Academy of Sciences of Ukraine, 1 Svientsitskii Street, L'viv-11, 79011, Ukraine*

³*Universitätsrechenzentrum, Universität Magdeburg, P.O. Box 4120, 39016 Magdeburg, Germany*

⁴*IESK, Kognitive Systeme, Universität Magdeburg, P.O. Box 4120, 39016 Magdeburg, Germany*

(Dated: October 24, 2018)

Using the coupled cluster method for high orders of approximation and complementary exact diagonalization studies we investigate the ground state properties of the spin-1/2 J_1 - J_2 frustrated Heisenberg antiferromagnet on the square lattice. We have calculated the ground-state energy, the magnetic order parameter, the spin stiffness, and several generalized susceptibilities to probe magnetically disordered quantum valence-bond phases. We have found that the quantum critical points for both the Néel and collinear orders are $J_2^{c1} \approx (0.44 \pm 0.01)J_1$ and $J_2^{c2} \approx (0.59 \pm 0.01)J_1$ respectively, which are in good agreement with the results obtained by other approximations. In contrast to the recent study by [Sirker et al. Phys. Rev. B **73**, 184420 (2006)], our data do not provide evidence for the transition from the Néel to the valence-bond solid state to be first order. Moreover, our results are in favor of the deconfinement scenario for that phase transition. We also discuss the nature of the magnetically disordered quantum phase.

I. INTRODUCTION

Quantum phase transitions between semiclassical magnetically ordered phases and magnetically disordered quantum phases which are driven by frustration attract much interest; see, e.g., Ref. 1. A canonical model for studying such transitions is the spin-1/2 Heisenberg antiferromagnet with nearest-neighbor J_1 and frustrating next-nearest-neighbor J_2 coupling (J_1 - J_2 model) on the square lattice. This model has attracted a great deal of interest during the last 20 years (see, e.g., Refs. 2,3,4,5,6,7,8,9,10,11,12,13,14,15,16,17,18,19,20,21,22,23,24,25,26,27,28,29,30,31 and references therein). Recent interest in this model comes also from the synthesis of layered magnetic materials $\text{Li}_2\text{VO}_2\text{SiO}_4$, $\text{Li}_2\text{VOGeO}_4$, VOMoO_4 , and $\text{BaCdVO}(\text{PO}_4)_2$ (Refs. 32,33,34,35) that might be described by the J_1 - J_2 model. A new promising perspective is also opened by the recently discovered layered Fe-based superconducting materials³⁶ which may have a magnetic phase that can be described by a J_1 - J_2 model with spin quantum number $s > 1/2$.^{37,38,39}

For the square-lattice spin-1/2 J_1 - J_2 model it is well accepted that there are two magnetically long-range ordered ground state (GS) phases at small and at large J_2 separated by an intermediate quantum paramagnetic phase without magnetic long-range order (LRO) in the parameter region $J_2^{c1} \leq J_2 \leq J_2^{c2}$, where $J_2^{c1} \approx 0.4J_1$ and $J_2^{c2} \approx 0.6J_1$. The magnetic phase at low $J_2 < J_2^{c1}$ exhibits semiclassical Néel LRO with a magnetic wave vector $\mathbf{Q}_0 = (\pi, \pi)$. The magnetic phase at large $J_2 > J_2^{c2}$ shows so-called collinear LRO. It is twofold degenerate and the corresponding magnetic wave vectors are $\mathbf{Q}_1 = (\pi, 0)$ or $\mathbf{Q}_2 = (0, \pi)$. These two collinear states are characterized by a parallel spin orientation of nearest neighbors in vertical (horizontal) direction and an

antiparallel spin orientation of nearest neighbors in horizontal (vertical) direction.

The nature of the transition between the Néel and the quantum paramagnetic phases as well as the properties of the quantum paramagnetic phase and the precise values of the transition points, is still under debate.^{2,3,4,5,6,7,8,9,10,11,12,13,14,15,16,17,18,19,20,21,22,23,24,25,26,27,28,29,30,} In particular, stimulated by the recent discussion of deconfined quantum criticality in two-dimensional spin systems,^{40,41} a renewed interest in the nature of the phase transition between the semiclassical Néel phase and the quantum paramagnetic phase has emerged.^{27,30,42,43} However, in spite of numerous intensive efforts focused on the transition between the Néel and the quantum paramagnetic phases in the J_1 - J_2 square-lattice antiferromagnet and some other candidate models,^{44,45,46,47,48,49} this field remains still highly controversial.

For completeness we mention that the classical square-lattice J_1 - J_2 model ($s \rightarrow \infty$) exhibits a direct first-order transition between Néel state and collinear state at $J_2/J_1 = 1/2$.

Recently, several extensions of J_1 - J_2 model have been studied. Interestingly, with increase in the space dimension from $D = 2$ to $D = 3$ the intermediate quantum paramagnetic phase disappears.^{29,50,51} Also spatial^{52,53,54,55,56} and spin anisotropies^{26,57,58} as well as the spin quantum number s (Refs. 2,30,59 and 60) have a great influence on the GS phase diagram.

The goal of this paper is to study the GS phase diagram for spin-half J_1 - J_2 model on the square lattice using a high-order coupled cluster method (CCM). We complement the CCM treatment by exact diagonalization (ED) for finite lattices for a qualitative check of our CCM data. By calculating GS quantities such as the energy, the magnetic order parameter, the spin stiffness and

generalized susceptibilities we will investigate the quantum phase transitions present in the model as well as the properties of the quantum paramagnetic phase. We will compare our results with the ones obtained recently using series expansions.²⁷

The CCM, introduced many years ago by Coester and Kummel,⁶¹ is one of the most universal and most powerful methods of quantum many-body theory. For a review of the CCM see, e.g., Ref. 62. Starting in 1990 it has been applied to quantum spin systems with much success.^{15,29,63,64,65,66,67,68,69,70,71,72,73,74,75} A main advantage of this approach consists in its applicability to strongly frustrated quantum spin systems in any dimension. With the implementation of parallelization in the CCM code^{72,76} high-order calculations are now possible (see Sec. II), improving significantly the accuracy in the investigation of quantum phase transitions driven by frustration.^{29,56,58,67,69,72,73,75}

The Hamiltonian of the considered J_1 - J_2 model reads

$$H = J_1 \sum_{\langle ij \rangle} \mathbf{s}_i \mathbf{s}_j + J_2 \sum_{[ij]} \mathbf{s}_i \mathbf{s}_j, \quad (1)$$

where J_1 is the nearest-neighbor exchange coupling and J_2 is the next-nearest-neighbor exchange coupling. Both couplings are antiferromagnetic, $J_1 > 0$ and $J_2 > 0$. In our CCM and ED calculations we set $J_1 = 1$. We consider spin quantum number $s = 1/2$, i.e., $\mathbf{s}_i^2 = 3/4$.

The remainder of the paper is organized as follows. In Sec. II we briefly discuss the CCM approach and illustrate how to calculate of GS quantities of spin model (1). We present our results for the GS energy, the magnetic order parameter and the spin stiffness in Sec. III A. In Sec. III B, we consider in more detail the phase transition between the Neel state and the quantum paramagnetic state as well as various susceptibilities testing the nature of the nonmagnetic phase. Finally, in Sec. IV we summarize our findings.

II. COUPLED CLUSTER METHOD

We start with a brief illustration of the main features of the CCM. For a general overview on the CCM the interested reader is referred, e.g., to Refs. 64,66,67,68,70 and 72,73,74. The starting point for a CCM calculation is the choice of a normalized model (or reference) state $|\Phi\rangle$, together with a set of mutually commuting multispin creation operators C_I^+ which are defined over a complete set of many-body configurations I . The operators C_I^- are the multispin destruction operators and are defined to be the Hermitian adjoint of the C_I^+ . We choose $\{|\Phi\rangle; C_I^+\}$ in such a way that we have $\langle \Phi | C_I^+ = 0 = C_I^- | \Phi \rangle$, $\forall I \neq 0$. Note that the CCM formalism corresponds to the thermodynamic limit $N \rightarrow \infty$.

For the spin system considered, for $|\Phi\rangle$ we choose the two-sublattice Neel state for small J_2 but the collinear state for large J_2 . To treat each site equivalently we

perform a rotation of the local axis of the spins such that all spins in the reference state align along the negative z axis. In the rotated coordinate frame then we have $|\Phi\rangle = |\downarrow\rangle|\downarrow\rangle|\downarrow\rangle \dots$ and the corresponding multispin creation operators then read $C_I^+ = s_i^+, s_i^+ s_j^+, s_i^+ s_j^+ s_k^+, \dots$, where the indices i, j, k, \dots denote arbitrary lattice sites.

The CCM parameterizations of the ket- and bra-ground states are given by

$$\begin{aligned} H|\Psi\rangle &= E|\Psi\rangle; & \langle \tilde{\Psi} | H &= E \langle \tilde{\Psi} |; \\ |\Psi\rangle &= e^S |\Phi\rangle, & S &= \sum_{I \neq 0} \mathcal{S}_I C_I^+; \\ \langle \tilde{\Psi} | &= \langle \Phi | \tilde{S} e^{-S}, & \tilde{S} &= 1 + \sum_{I \neq 0} \tilde{\mathcal{S}}_I C_I^-. \end{aligned} \quad (2)$$

The correlation operators S and \tilde{S} contain the correlation coefficients \mathcal{S}_I and $\tilde{\mathcal{S}}_I$ that have to be determined. Using the Schrodinger equation, $H|\Psi\rangle = E|\Psi\rangle$, we can now write the GS energy as $E = \langle \Phi | e^{-S} H e^S | \Phi \rangle$. The magnetic order parameter is given by

$$M = -\frac{1}{N} \sum_{i=1}^N \langle \tilde{\Psi} | s_i^z | \Psi \rangle, \quad (3)$$

where s_i^z is expressed in the rotated coordinate system. To find the ket-state and bra-state correlation coefficients we require that the expectation value $\bar{H} = \langle \tilde{\Psi} | H | \Psi \rangle$ is a minimum with respect to the bra-state and ket-state correlation coefficients, such that the CCM ket- and bra-state equations are given by

$$\begin{aligned} \langle \Phi | C_I^- e^{-S} H e^S | \Phi \rangle &= 0, & \forall I \neq 0, & \quad (4) \\ \langle \Phi | \tilde{S} e^{-S} [H, C_I^+] e^S | \Phi \rangle &= 0, & \forall I \neq 0. & \quad (5) \end{aligned}$$

Each ket- or bra-state [Eq. 4) or (5)] belongs to a particular index I corresponding to a certain set (configuration) of lattice sites i, j, k, \dots in the multispin creation operator $C_I^+ = s_i^+, s_i^+ s_j^+, s_i^+ s_j^+ s_k^+, \dots$; see above.

Though we start our CCM calculation with a reference state corresponding to semiclassical order, one can compute the GS energy also in parameter regions where semiclassical magnetic LRO is destroyed, and it is known^{15,29,56,58,67,72,73} that the CCM yields precise results for the GS energy beyond the transition from the semiclassical magnetic phase to the quantum paramagnetic phase. The necessary condition for the convergence of the CCM equations is a sufficient overlap between the reference state and the true ground state.

It has been recently demonstrated⁷⁴ that the CCM can also be used to calculate the spin stiffness ρ_s with high accuracy. The stiffness measures the increase in the amount of energy when we twist the magnetic order parameter of a magnetically long-range ordered system along a given direction by a small angle θ per unit length, i.e.

$$\frac{E(\theta)}{N} = \frac{E(\theta=0)}{N} + \frac{1}{2} \rho_s \theta^2 + \mathcal{O}(\theta^4), \quad (6)$$

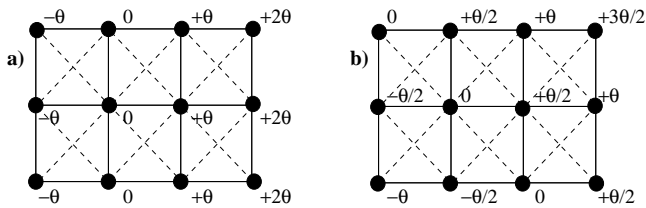


FIG. 1: Illustration of the twisted reference states used for the calculation of the spin stiffness ρ_s . The angles at the lattice sites indicate the twist of the spins with respect to the Néel or the collinear state. (a): Twisted Néel state; the twist is introduced along rows in x direction. (b): Twisted collinear state; the twist is introduced along rows in $\vec{e}_x + \vec{e}_y$ direction.

where $E(\theta)$ is the GS energy as a function of the imposed twist, and N is the number of sites. In the thermodynamic limit, a positive value of ρ_s means that there is magnetic LRO in the system, while a value of zero reveals that there is no magnetic LRO. To calculate the spin stiffness within the CCM using Eq. (6) we must modify the corresponding reference states (Néel or collinear) by introducing an appropriate twist θ , see Fig. 1. Thus the ket-state correlation coefficients S_I [after solving CCM equation (4)] depend on θ and, hence, the GS energy E is also dependent on θ .

To study the properties of the quantum paramagnetic phase existing in the vicinity of $J_2 = J_1/2$ as well as the phase transitions to that phase we will consider generalized susceptibilities χ_F that describe the response of the system to certain "field" operator F .^{17,18,20,22,23,27} To calculate such a susceptibility χ_F we add to Hamiltonian (1) a field term $F = \delta \hat{O}$, where \hat{O} is an operator that breaks some symmetry of H and the coefficient δ determines the strength of the field. Using the CCM with either the Néel or the collinear reference state we calculate the energy per site $E(\delta)/N = e(\delta)$ for $H + F$, i.e., for the Hamiltonian of Eq. (1) perturbed by the additional term $\delta \hat{O}$. The susceptibility χ_F is then defined as

$$\chi_F = - \left. \frac{\partial^2 e(\delta)}{\partial \delta^2} \right|_{\delta=0}. \quad (7)$$

For the considered quantum spin model we have to use approximations in order to truncate the expansion of S and \tilde{S} . We use the well elaborated LSUB n scheme^{64,66,68,70,73} in which in the correlation operators S and \tilde{S} one takes into account all multispin correlations over all distinct locales on the lattice defined by n or fewer contiguous sites. For instance, within the LSUB4 approximation one includes multispin creation operators of one, two, three or four spins distributed on arbitrary clusters of four contiguous lattice sites. The number of these fundamental configurations can be reduced exploiting lattice symmetry and conservation laws. In the CCM-LSUB10 approximation we have finally 29605 (45825) fundamental configurations for the Néel (collinear) reference state. Note, however, that for the calculation of

the stiffness (the susceptibilities) the twisted reference state (the modified Hamiltonian $H + F$) is less symmetric, which leads to more fundamental configurations. As a result we are then limited to LSUB8 approximation.

Since the LSUB n approximation becomes exact for $n \rightarrow \infty$, it is useful to extrapolate the "raw" LSUB n data to $n \rightarrow \infty$. Meanwhile there is a great deal of experience how to extrapolate the GS energy e and the magnetic order parameter M . Most successful are the parameter fits of the form $A(n) = A_0 + A_1(1/n)^{\nu_1} + A_2(1/n)^{\nu_2}$ where the fixed leading exponents ν_1 and ν_2 may be different for the different quantities to be extrapolated. For the GS energy per spin $e(n) = a_0 + a_1(1/n)^2 + a_2(1/n)^4$ is a reasonable well-tested extrapolation ansatz.^{29,56,58,67,68,70,72,73} An appropriate extrapolation rule for the magnetic order parameter for systems showing a GS order-disorder transition is^{56,58,59,75} $M(n) = b_0 + b_1(1/n)^{1/2} + b_2(1/n)^{3/2}$. For the spin stiffness the extrapolation $\rho_s(n) = c_0 + c_1(1/n) + c_2(1/n)^2$ has been found to be reasonable.⁷⁴ Finally, for the susceptibility we have tested several fitting functions, and we have found that the best extrapolation is obtained by the same fitting function $\chi_F(n) = c_0 + c_1(1/n) + c_2(1/n)^2$ as for the stiffness. To check the reliability of this extrapolation scheme we have also performed an extrapolation of the energy $e(\delta)$ to $n \rightarrow \infty$ by using the extrapolation formula $e(n) = a_0 + a_1(1/n)^2 + a_2(1/n)^4$ (see above) and a subsequent calculation of χ_F according to Eq. (7) using the extrapolated energy. We found that the deviations between both schemes are very small.

In summary, the CCM approach automatically implies the thermodynamic limit $N \rightarrow \infty$ (that is an obvious advantage in comparison with ED). However, we need to extrapolate to the $n \rightarrow \infty$ limit in the truncation index n , which is an internal parameter of the approach. Since no general theory is known how the physical quantities scale with n , we have to use extrapolation formulas based on empirical experience. Another feature of many approximate techniques (but not of ED) is that they are based on reference states explicitly breaking some symmetry of the Hamiltonian. Although CCM also starts from a reference state related to a particular magnetic LRO, it has been demonstrated that the CCM provides precise results for the GS energy even in parameter regions where the magnetic LRO (i.e., the magnetic order parameter M calculated within CCM) vanishes.^{15,29,56,58,67,72,73} This is again an advantage of the CCM approach.

III. GROUND-STATE PHASE DIAGRAM

A. Ground state energy, magnetic order parameter and spin stiffness

As already mentioned in Sec. I, the considered J_1 - J_2 model has two semiclassical magnetic GS phases (small and large J_2) separated by nonmagnetic quantum phase (intermediate J_2). To detect the quantum critical points

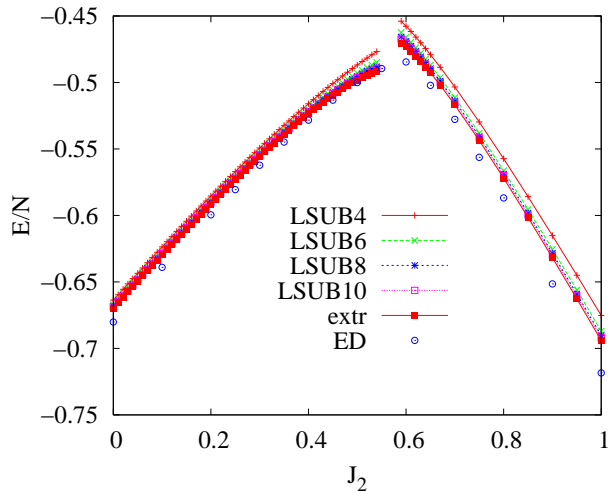


FIG. 2: (Color online) The GS energy per spin as function of J_2 obtained by CCM-LSUB n with $n = 4, 6, 8, 10$ and its extrapolated values to $n \rightarrow \infty$ using the extrapolation scheme $e(n) = a_0 + a_1(1/n)^2 + a_2(1/n)^4$. ED results for $N = 32$ are shown by circles.

by the above described CCM we discuss the magnetic order parameter M [see Eq. (3)], and the spin stiffness ρ_s [see Eq. (6)]. Both, M and ρ_s , are finite in the magnetically ordered phases but vanish in the intermediate quantum paramagnetic phase.

For completeness, we show first the CCM and the ED GS energies per spin, $e = E/N$, in Fig. 2. The CCM curve consists of two parts corresponding to the Néel and collinear reference states, respectively. The dependence $e(J_2)$ for ED and CCM is qualitatively the same; however, due to finite-size effects, the ED curve is below the CCM curves. Let us mention again that CCM GS energy corresponding to the Néel (collinear) reference state is expected to be precise also in the intermediate quantum paramagnetic phase if J_2 is not too far beyond the transition points.

Next we consider the magnetic order parameter in dependence on J_2 , see Fig. 3. Note again that only for the magnetic order parameter M and the GS energy we are able to solve the CCM-LSUB n equations up to $n = 10$, while for the stiffness and the susceptibilities we are restricted to $n \leq 8$. Hence the extrapolation to the limit $n \rightarrow \infty$ is most reliable for M and the estimation of the phase transition points by using the data for M is most accurate. The extrapolation to $n \rightarrow \infty$ shown in Fig. 3 is based on the extrapolation scheme $M(n) = b_0 + b_1(1/n)^{1/2} + b_2(1/n)^{3/2}$ and uses CCM-LSUB n data with $n = 4, 6, 8, 10$. We find for the phase transition points between the semiclassical phases and the quantum paramagnetic phase $J_2^{c1} = 0.447J_1$ and $J_2^{c2} = 0.586J_1$. To check the robustness of this extrapolation we have also extrapolated M using the data of $n = 2, 4, 6, 8, 10$ which leads to $J_2^{c1} = 0.443J_1$ and

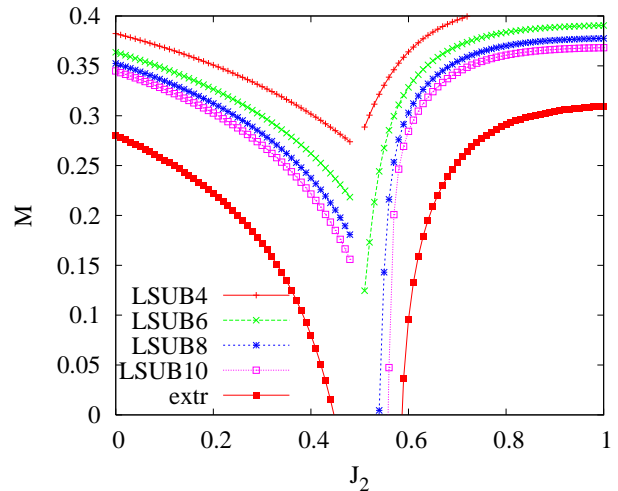


FIG. 3: (Color online) Magnetic order parameter M versus J_2 obtained by CCM-LSUB n with $n = 4, 6, 8, 10$ and its extrapolated values to $n \rightarrow \infty$ using the extrapolation scheme $M(n) = b_0 + b_1(1/n)^{1/2} + b_2(1/n)^{3/2}$.

$J_2^{c2} = 0.586J_1$. Those values J_2^{c1} and J_2^{c2} are in agreement with CCM predictions of Refs. 56 and 58.

Although the behavior of the extrapolated values of the magnetic order parameter around J_2^{c1} and J_2^{c2} presented in Fig. 3 shows a continuous behavior near J_2^{c1} and near J_2^{c2} , it is obvious that the decay of the collinear order parameter to zero at J_2^{c2} is much steeper than the decay of the Néel order parameter at J_2^{c1} . That might give some hint of a first-order phase transition from the collinear to the paramagnetic phase, in contrast to a continuous transition from the Néel to the paramagnetic phase.^{6,16,20}

In addition to the magnetic order parameter, another way to find the phase transition points is to consider the spin stiffness ρ_s which is nonzero in a magnetically long-range ordered phase but vanishes in the magnetically disordered quantum phase. The spin stiffness measures the distance of the ground state from criticality,⁷⁷ and constitutes together with the spin-wave velocity the fundamental parameters that determines the low-energy dynamics of magnetic systems.^{78,79,80} In order to calculate the stiffness directly using Eq. (6) we have to modify both the reference (Néel and collinear) states by introducing an appropriate twist θ ; see Fig. 1. The CCM LSUB n results for spin stiffness as well as the extrapolated values for both reference states as a function of J_2 are given in Fig. 4. The results show that approaching the magnetically disordered phase the stiffness is decreased until it vanishes at $J_2 = 0.466J_1$ coming from the Néel phase and at $J_2 = 0.578J_1$ coming from the collinear phase. These values obtained by extrapolation including up to LSUB8 data are in reasonable agreement with the critical points determined by extrapolating M . Note that our data for ρ_s are also in good agreement with corresponding results of the other methods (see Refs. 7,12,14 and 81). Note

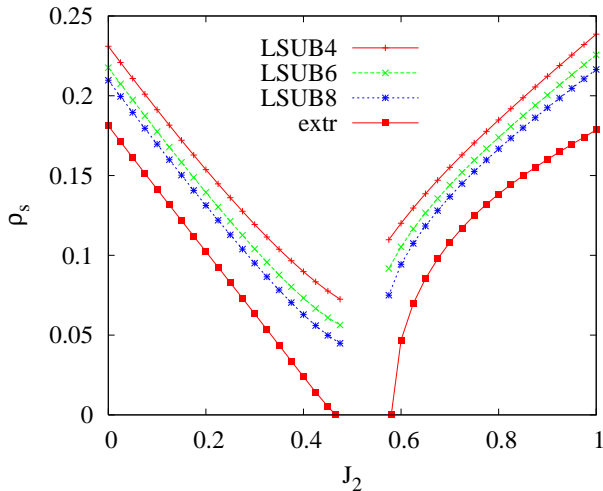


FIG. 4: (Color online) The spin stiffness ρ_s versus J_2 obtained by CCM-LSUB n with $n = 4, 6, 8$ and its extrapolated values to $n \rightarrow \infty$ using the extrapolation scheme $\rho_s(n) = c_0 + c_1(1/n) + c_2(1/n)^2$.

further that similarly as for M we observe also for ρ_s that the curvature near the critical points is different at J_2^{c1} and at J_2^{c2} that might be again a hint of the different nature of both transitions.

To summarize, the CCM results for the GS energy, the magnetic order parameter, and the spin stiffness support a general physical picture known from earlier numerical studies (including ED,^{3,4,6,9,10} variational quantum Monte Carlo,^{17,21} and series expansions^{22,27}). For intermediate values of J_2 , $J_2^{c1} \leq J_2 \leq J_2^{c2}$ with $J_2^{c1} \approx (0.44 \pm 0.01)J_1$ and $J_2^{c2} \approx (0.59 \pm 0.01)J_1$ there is no magnetic order.

B. Order of the phase transition: Generalized susceptibilities

While the phase transition from the collinear to the paramagnetic phase is most likely of first order,^{6,16,20} concerning the nature of phase transition from the Néel to the paramagnetic phase so far no conclusive answers are known. However, the question about the order of the phase transition from the Néel to the paramagnetic phase is of great interest in particular in connection with the validity of the Landau-Ginzburg paradigm.^{40,41} Very recently a number of arguments by Sirker et al.²⁷ based on series expansions and spin-wave theory were given that this transition is of first order. We reconsider this issue below using CCM and complementary ED results.

The first type of arguments in favor of the first-order phase transition from the Néel to the paramagnetic phase presented in Ref. 27 was based on the combination of field theory with series-expansion data. In what follows we use the same approach as that of Sirker et al.;²⁷ however,

instead of series-expansion data we use CCM and ED data. Interestingly, we will arrive at a different conclusion concerning the nature of the phase transition.

The second type of arguments supporting the first-order phase transition from the Néel to the paramagnetic phase were based on series-expansion data for several susceptibilities that test a possible valence-bond solid (VBS) order in the paramagnetic phase. In what follows we use the CCM and ED to compute four different susceptibilities χ_j defined in Eq. (7) for the J_1 - J_2 model. The corresponding perturbations (fields) $F_j = \delta \hat{O}_j$, $j = 1, \dots, 4$, are given by

$$F_1 = \delta \sum_{i,j} (-1)^i \mathbf{s}_{i,j} \mathbf{s}_{i+1,j}, \quad (8)$$

$$F_2 = \delta \sum_{i,j} (\mathbf{s}_{i,j} \mathbf{s}_{i+1,j} - \mathbf{s}_{i,j} \mathbf{s}_{i,j+1}), \quad (9)$$

$$F_3 = \delta \sum_{i,j} (-1)^{i+j} (s_{i,j}^x s_{i+1,j+1}^x + s_{i,j}^y s_{i+1,j+1}^y), \quad (10)$$

$$F_4 = \delta \sum_{i,j} [(-1)^i \mathbf{s}_{i,j} \mathbf{s}_{i+1,j} + (-1)^j \mathbf{s}_{i,j} \mathbf{s}_{i,j+1}], \quad (11)$$

where i, j are components (integer numbers) of the lattice vectors of the square lattice [see Fig. 5], where we visualize perturbation terms (8) – (11). The above definitions, Eqs. (8) – (11), are in accordance with previous discussions^{17,20,22,23} and²⁷ of possible valence-bond states or broken symmetries in the magnetically disordered quantum phase. Previous results for χ_1 can be found in Refs. 17,20,22,23 and 27, for χ_2 in Refs. 17 and 27, and for χ_3 in Refs. 22 and 27. Note that in Refs. 22 and 27 the results for the perpendicular χ_3 [i.e., the field $F_3 = \delta \hat{O}_3$ contains only x and y components, see Eq. (10)] were reported only. For reasons of comparison with the available series-expansion data we consider in the present study also the perpendicular χ_3 . To our best knowledge so far no data for the susceptibility χ_4 are published.⁸²

Note that all susceptibilities defined by Eqs. (8) – (11) break the symmetry of the initial square lattice, for details, see Refs. 17,20,22,23 and 27. The susceptibilities χ_1 and χ_4 are most interesting, since they belong to order-parameter operators \hat{O}_1 and \hat{O}_4 probing directly possible valence-bond ordering. As discussed in Ref. 41 they can also be interpreted as a single complex order parameter with a different phase for the two patterns. Note that for the field F_1 we have chosen the x -axis for the alignment of modified nearest-neighbor bonds, see Fig. 5a. Alternatively, the y -axis can be chosen. It is worth mentioning that the field F_4 [Eq. 11] is a sum of fields F_1 aligned along x and y axes, i.e., $F_4 = F_1^{(x)} + F_1^{(y)}$, and hence $\chi_4 = \chi_1^{(x)} + \chi_1^{(y)}$. If, in addition, a symmetry with respect to a $\pi/2$ -rotation in the square-lattice plane holds

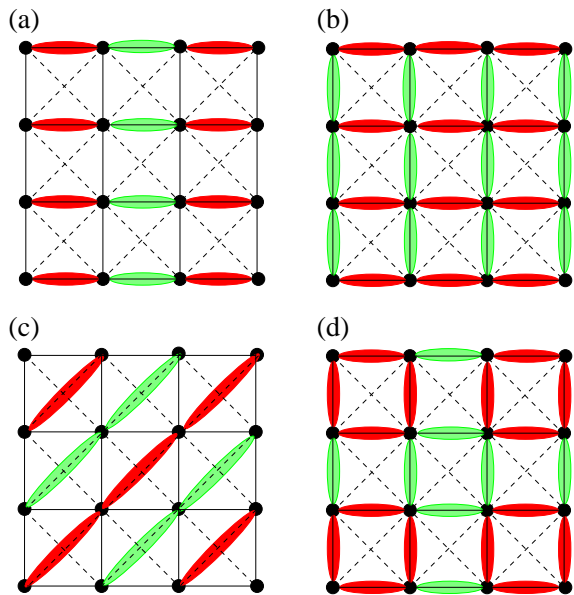


FIG. 5: (Color online) Illustration of perturbations (fields) F_j related to generalized susceptibilities χ_j : (a) perturbation F_1 (8), (b) perturbation F_2 (9), (c) perturbation F_3 (10) and (d) perturbation F_4 (11). Dark (red) [light (green)] shadows correspond to enforced [weakened] exchange couplings.

(that is, however, not the case, e.g., for the CCM calculations for large J_2), one has $\chi_1^{(x)} = \chi_1^{(y)}$ and $\chi_4 = 2\chi_1$.

Analyzing the behavior of the susceptibilities as J_2 approaches the critical value J_2^{c1} we will again arrive at a different conclusion in comparison to that in Ref. 27.

We begin with the examination of the order of the phase transition from the Néel to the VBS state. In contrast to the transition from the VBS to the collinear state where an energy level crossing indicates a first-order transition,^{16,27,56} the energy behaves smoothly as J_2 varies around J_2^{c1} and a more sensitive method for distinguishing between first- and second-order transitions has to be applied.²⁷ For that we consider the GS energy $e(\delta)$ for Hamiltonian (1) perturbed by the field $F_1 = \delta\hat{O}_1$ [Eq. 8]. We have performed CCM calculations for $e(\delta)$ choosing the Néel state as the reference state and extrapolating LSUB n data with $n = 4, 6, 8$ according to the scaling law $e(n) = a_0 + a_1(1/n)^2 + a_2(1/n)^4$ [see Fig. 6a]. We have also performed complementary ED for a finite square lattice of $N = 32$ sites [see Fig. 6b] for a qualitative check of the CCM results. The obtained dependence $e(\delta)$ may be fitted for a fixed J_2 to the following polynomial form

$$e(\delta) - e(0) = \frac{a}{2}\delta^2 + \frac{b}{4}\delta^4 + \frac{c}{6}\delta^6. \quad (12)$$

To determine the order of the phase transition we use the method described in Ref. 27. For a two-dimensional antiferromagnet, the system could be described by the

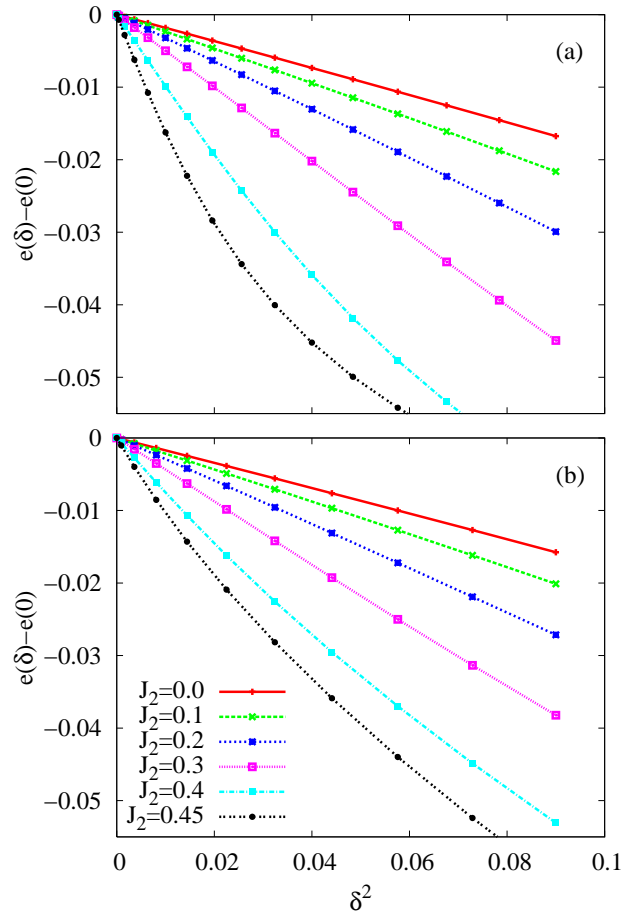


FIG. 6: (Color online) The GS energy $e(\delta) - e(0)$ versus square of field strength δ for $H + \delta\hat{O}_1$ [see Eq. (8)], for $J_2 = 0.0, 0.1, 0.2, 0.3, 0.4$ and 0.45 (from top to bottom). (a): CCM results extrapolated to $n \rightarrow \infty$ using the extrapolation scheme $e(n) = a_0 + a_1(1/n)^2 + a_2(1/n)^4$. (b): ED results for $N = 32$. The displayed curves might be compared to the ones in Fig. 1 of Ref. 27 where corresponding series-expansion data for $e(\delta)$ are reported (however, only up to $J_2 = 0.3$).

following $O(3)$ model:

$$H_v = \frac{1}{2} \left[(\partial_t \vec{v})^2 + c_v^2 (\vec{\nabla} \vec{v})^2 + m_v^2 \vec{v}^2 \right] + \frac{u_v}{4} (\vec{v}^2)^2. \quad (13)$$

Consider now the case that we are in the magnetically ordered phase and add the field F_1 [Eq. 8] with $|\delta| \ll 1$. The Néel order will then coexist with a small dimerization described by a scalar field

$$H_\phi = \frac{1}{2} \left[(\partial_t \phi)^2 + c_\phi^2 (\vec{\nabla} \phi)^2 + m_\phi^2 \phi^2 \right] + \frac{u_\phi}{4} \phi^4 + \frac{r_\phi}{6} \phi^6 - \delta \phi. \quad (14)$$

The fields \vec{v} and ϕ are not independent, and the interaction between them reads

$$H_{\text{int}} = \frac{u_{v\phi}}{2} \vec{v}^2 \phi^2. \quad (15)$$

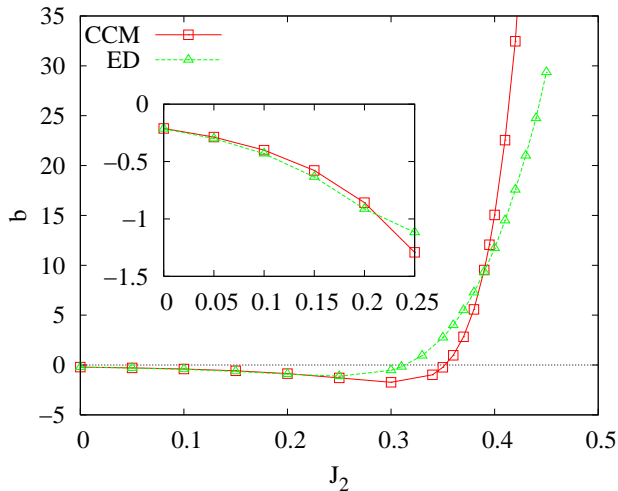


FIG. 7: (Color online) The coefficient b of the quartic term in Eq. (12) obtained from a fit of the CCM data in Fig. 6a and the ED data in Fig. 6b in dependence on J_2 . This figure might be compared to Fig. 3 of Ref. 27. Inset: the coefficient b versus J_2 shown for small J_2 with an enlarged scale.

The effective field theory in the ordered phase for $\delta \neq 0$ is then given by $H = H_v + H_\phi + H_{\text{int}}$. Combining Eqs. (13)-(15) we will have a nonzero GS expectation value

$$\langle \phi \rangle = \frac{\delta}{A} - \frac{u_\phi}{A^4} \delta^3 + \frac{3u_\phi^2 - Ar_\phi}{A^7} \delta^5 + \mathcal{O}(\delta^7), \quad (16)$$

with $A = m_\phi^2 + u_{v\phi} \langle \vec{v} \rangle^2$. Equation (16) leads to a GS energy given by

$$e(\delta) - e(\delta = 0) = -\frac{1}{2A} \delta^2 + \frac{u_\phi}{4A^4} \delta^4 + \frac{Ar_\phi - 3u_\phi^2}{6A^7} \delta^6 + \mathcal{O}(\delta^8). \quad (17)$$

The coefficient of the δ^4 term in Eq. (17) may be positive or negative depending on the sign of the parameter u_ϕ . In the case of $u_\phi > 0$ we have a second-order transition with respect to ϕ at a critical point, and a first-order transition if $u_\phi < 0$.

Using the polynomial in Eq. (12) we have fitted the data of $e(\delta)$, $\delta^2 = 0 \dots 0.09$ for various J_2 including values near the critical point J_2^{c1} [see Fig. 6a]. We find that the coefficient of the δ^4 -term b is negative for small values of J_2 but becomes positive if J_2 approaches J_2^{c1} ; see Fig. 7. This behavior is found for the CCM data as well as for the ED data. In particular, b calculated by the CCM (calculated by the ED) changes its sign at $J_2 \approx 0.35$ (at $J_2 \approx 0.31$).

Comparing Fig. 7 with the results reported in Fig. 3 of Ref. 27 we note that CCM data for J_2 below 0.2 are in reasonable agreement with series expansions, linear spin-wave theory, or mean field spin-wave theory [in particular, CCM yields $b(J_2 = 0.1) \approx -0.40$, $b(J_2 = 0.2) \approx -0.86$, $b(J_2 = 0.25) \approx -1.29$, $b(J_2 = 0.3) \approx -1.73$ that is in between the series-expansion data and the spin-wave theory results]. A drastic difference between the

series-expansion data and the CCM results emerges if J_2 approaches the critical value J_2^{c1} : The series expansion gives $b < 0$ whereas the CCM and the ED yield $b > 0$ for $J_2 \rightarrow J_2^{c1}$. We recall that any predictions from spin-wave theory for the considered J_1 - J_2 model are likely to be unreliable if J_2 exceeds 0.35.⁸ Combining Eqs. (12) and (17) we get $b = u_\phi a^4$ and determining a and b using CCM data (Fig. 6a) for $J_2 = 0.36 \dots 0.42$ we find $u_\phi \approx 0.75 > 0$.

In summary, the presented CCM and ED data, in contrast to series-expansion data of Ref. 27, do not support a weak first-order phase transition from the Néel to the VBS state²⁷ but give evidence that this transition is continuous.

Next we examine the susceptibilities associated with probing fields (8) – (11) directly. The CCM results are shown in Fig. 8. We also present in this figure the ED data for $N = 16, 24$, and 32 lattice in the insets. (We do not show $N = 24$ results for χ_1 and χ_2 since the system of rectangular shape perturbed by F_1 or F_2 does not possess symmetry with respect to a $\pi/2$ rotation in the square-lattice plane.) Note that a sophisticated finite-size analysis has to be performed in order to derive the correct behavior of susceptibilities in the thermodynamic limit.¹⁷ Such an analysis goes beyond the scope of the present study since we use the ED data as a qualitative check of our CCM results only. We notice here that although χ_1 and χ_4 are related to each other (see above), they are calculated completely independently. We have confirmed the expected relation between these susceptibilities thus providing an additional double check for our numerics.

As it has been already mentioned above, the susceptibilities χ_1 , χ_2 , and χ_3 were calculated in earlier studies using different methods. Our CCM results for χ_1 and χ_2 are in a good quantitative agreement with series-expansion results reported for $J_2 = 0 \dots 0.5$ in Refs. 20 and 27. [For instance, one can compare our CCM data, $1/\chi_1(J_2 = 0.3) \approx 0.92$, $1/\chi_1(J_2 = 0.35) \approx 0.66$, and $\chi_2(J_2 = 0.3) \approx 0.90$, $\chi_2(J_2 = 0.35) \approx 1.06$, with the data shown in Figs. 2 and 5 of Ref. 27.] The CCM results for χ_1 and χ_2 also qualitatively agree with variational quantum Monte Carlo method and ED results reported (for some J_2 only) in Ref. 17. The CCM results for χ_3 , however, exhibit a different qualitative dependence on J_2 as J_2 approaches J_2^{c1} in comparison with series-expansion data.^{22,27} Compare, e.g., Fig. 6 of Ref. 27 and Fig. 8c of the present paper. According to series-expansion data χ_3 decreases by about 20% as J_2 increases from 0 to 0.4. In contrast, according to CCM data shown in Fig. 8c χ_3 increases by a factor of about 4 as J_2 increases from 0 to 0.4.

Let us now discuss some general features of the generalized susceptibilities shown in Fig. 8. Obviously, a divergence of a certain susceptibility (or $1/\chi \rightarrow 0$) at a particular value of J_2 indicates an instability of a GS phase regarding to a possible different GS order. It can be seen from Fig. 8, that all susceptibilities increase with

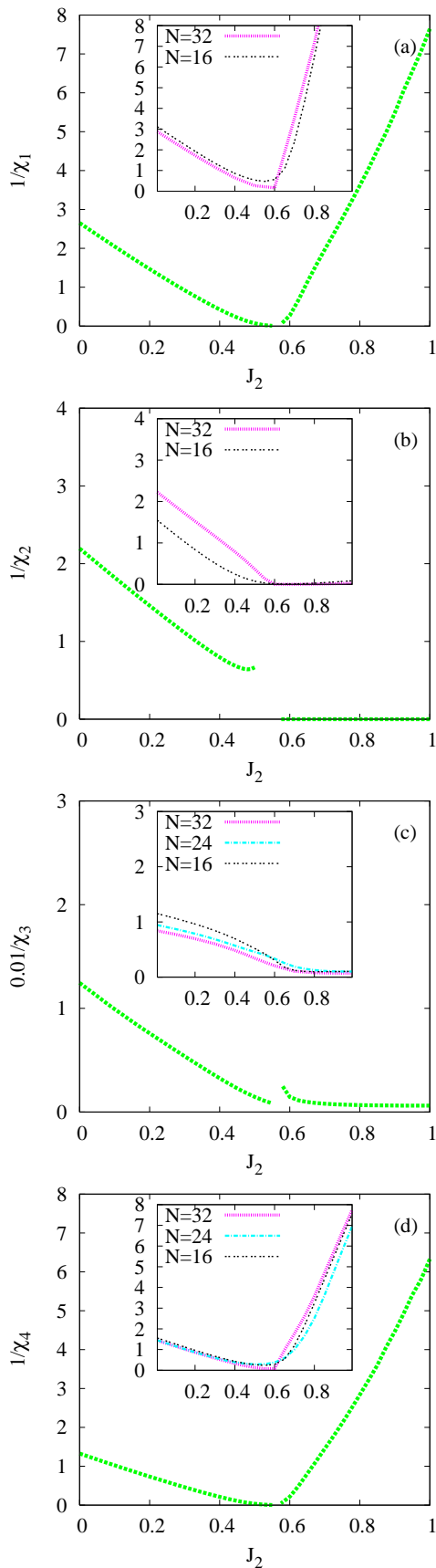


FIG. 8: (Color online) The inverse susceptibilities (a) $1/\chi_1$, (b) $1/\chi_2$, (c) $1/\chi_3$ (please note the scaling factor 0.01 at the y -axis), and (d) $1/\chi_4$ versus J_2 obtained within the CCM LSUB n approximation with $n = 4, 6, 8$ and extrapolated to $n \rightarrow \infty$ using $\chi(n) = c_0 + c_1(1/n) + c_2(1/n)^2$. Insets: the same as in the main panels but using ED for finite lattices of $N = 16, 24$, and 32 . Panel (a) might be compared to Fig. 2 of

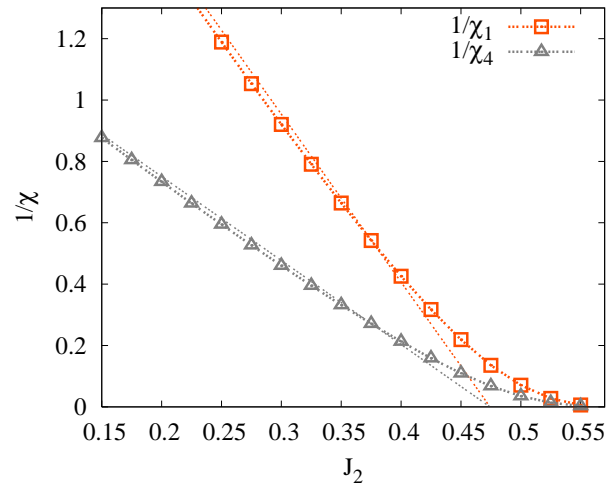


FIG. 9: (Color online) Susceptibilities $1/\chi_1$ (red) and $1/\chi_4$ (gray) around the critical point J_2^{c1} . Bold curves correspond to the CCM curves shown in Figs. 8a and 8d. Thin lines obtained from a linear fit of the CCM data for $0 \leq J_2 \leq J_2^{c1}$. Extrapolated (thin) lines become zero at $J_2 \approx 0.47$.

growing J_2 in the Néel phase. Near the critical point J_2^{c1} both $1/\chi_1$ and $1/\chi_4$ (CCM data imply $\chi_4 = 2\chi_1$) are significantly smaller than $1/\chi_2$ and $1/\chi_3$, indicating that the valence-bond states belonging to the columnar dimerized and plaquette patterns are favorable in the magnetically disordered quantum phase.

A similar behavior of χ_1 and χ_4 (CCM data imply $\chi_4 = \chi_1^{(x)} + \chi_1^{(y)}$) is observed if J_2 approaches J_2^{c2} from the collinear phase, i.e., from $J_2 > J_2^{c2}$. On this side the behavior of χ_2 and χ_3 is not conclusive, since both are already large in the collinear phase.

The behavior of the susceptibilities χ_1 and $\chi_4 (= 2\chi_1)$ near the critical point J_2^{c1} is shown in more detail in Fig. 9. Obviously, approaching J_2^{c1} from the Néel phase, χ_1 (χ_4) becomes very large; it however, remains finite in the region around J_2^{c1} up to $J_2 = 0.55$. That might be attributed to limited accuracy of CCM results since: (i) we have data only up to LSUB8 for extrapolation and (ii) LSUB n data based on the Néel reference state may become less accurate for values of J_2 exceeding J_2^{c1} . However, if the phase transition with respect to the corresponding VBS order parameter characterizing the quantum paramagnetic phase would be of second order we may expect an almost linear decrease in the inverse susceptibility if J_2 approaches J_2^{c1} , i.e., $1/\chi_1 \propto (J_2^{c1} - J_2)^{\gamma_\phi}$ with $\gamma_\phi \approx 1$.²⁷ Hence a linear fit of the CCM data of $1/\chi_1$ ($1/\chi_4$) versus J_2 using data points only within the Néel ordered region $0 \leq J_2 \leq J_2^{c1}$ might give reasonable results. We find that the linear fit for $1/\chi_1$ ($1/\chi_4$) vanishes at the point $J_2 \approx 0.47J_1$; see Fig. 9. This is in agreement with the scenario of deconfined criticality that predicts such divergence if the deconfined critical point is approached from the Néel phase.^{27,41}

To conclude this part, the CCM and ED data for all examined susceptibilities, χ_1 , χ_2 , χ_3 , and χ_4 , exhibit an enhancement while the system runs out of the Néel phase. This enhancement is most pronounced for χ_1 (χ_4). Moreover, χ_1 (χ_4) diverges at a value of J_2 close to the quantum critical point $J_2^{c1} \approx (0.44 \pm 0.01)J_1$ determined by the most accurate data for the Néel order parameter M . This finding is consistent with the predictions for a deconfined quantum critical point.⁴¹ Furthermore we find that our CCM data for χ_1 and χ_2 agree with the series-expansion data.²⁷ In contrast, for χ_3 we observe a qualitatively different behavior. Finally, the enhancement or divergence of the considered susceptibilities if J_2 approaches J_2^{c1} indicates that the translational symmetry is broken in the quantum paramagnetic phase, i.e. most likely a spatially homogeneous spin-liquid phase for $J_2^{c1} < J_2 < J_2^{c2}$ can be excluded.

IV. SUMMARY

To summarize, in this paper we have applied the CCM in high orders of approximation to the spin-1/2 J_1 - J_2 Heisenberg antiferromagnet on the square lattice and present a comprehensive analysis of the GS phase diagram of the model. For this purpose we have calculated the GS energy, the magnetic order parameter, the spin stiffness and several generalized susceptibilities. Our results enrich the list of available data and are complementary to other existing results obtained using different approximate methods such as series expansions or variational quantum Monte Carlo for the spin-1/2 J_1 - J_2 square-lattice Heisenberg antiferromagnet. In addition to the CCM results we present also ED results that are found to be in good agreement with the CCM data.

Our findings confirm the basic picture discussed earlier: For intermediate values of $J_2^{c1} \leq J_2 \leq J_2^{c2}$ the ground

state is a paramagnetic quantum state. The CCM prediction for the boundaries of the paramagnetic region is $J_2^{c1} \approx (0.44 \pm 0.01)J_1$ and $J_2^{c2} \approx (0.59 \pm 0.01)J_1$. To discuss the nature of the quantum phase transition from the semiclassical Néel phase to the quantum paramagnetic state at J_2^{c1} we use the CCM (and ED) data as an input for the method developed in Ref. 27 to distinguish between a first- and a second-order transition. Our analysis leads to the conclusion that the phase transition from the Néel to the paramagnetic state at J_2^{c1} is second order. This outcome contradicts the conclusion of Ref. 27 based on series-expansion data, but agrees with the deconfined critical point scenario proposed in Refs. 40 and 41.

Another way to check the predictions of the theory of deconfined quantum criticality is to examine the susceptibilities related to order parameters of a possible VBS ordering emerging, if the critical point is approached from the magnetically ordered Néel phase. The obtained data shown in Figs. 8 and 9 give another hint that χ_1 (χ_4) diverges at J_2^{c1} which does not contradict the deconfined critical point scenario.^{40,41}

Finally, the divergence or enhancement of the generalized susceptibilities obtained by CCM and ED approaching J_2^{c1} from the Néel phase gives evidence in favor of ground states breaking translational symmetry. Therefore, our data yield further arguments against a structureless (i.e., a spatially homogeneous) spin-liquid state without any LRO.

Acknowledgments

We thank O. Sushkov for interesting discussions. The research was supported by the DFG (Projects No. Ri615/16-1 and No. Ri615/18-1). O.D. acknowledges the kind hospitality of the University of Magdeburg in the spring of 2008.

-
- ¹ S. Sachdev, *Quantum Phase Transitions* (Cambridge University Press, 1999); S. Sachdev, in *Quantum Magnetism*, Lecture Notes in Physics Vol. **645**, edited by U. Schollwöck, J. Richter, D. J. J. Farnell, and R. F. Bishop, (Springer, Berlin, 2004), p. 381.
- ² P. Chandra and B. Douçot, Phys. Rev. B **38**, 9335 (1988).
- ³ E. Dagotto and A. Moreo, Phys. Rev. Lett. **63**, 2148 (1989).
- ⁴ F. Figueirido, A. Karlhede, S. Kivelson, S. Sondhi, M. Roček, and D. S. Rokhsar, Phys. Rev. B **41**, 4619 (1990).
- ⁵ N. Read and S. Sachdev, Phys. Rev. Lett. **66**, 1773 (1991).
- ⁶ H. J. Schulz and T. A. L. Ziman, Europhys. Lett. **18**, 355 (1992); H. J. Schulz, T. A. L. Ziman, and D. Poilblanc, J. Phys. I **6**, 675 (1996).
- ⁷ N. B. Ivanov and P. Ch. Ivanov, Phys. Rev. B **46**, 8206 (1992).
- ⁸ J.-i. Igarashi, J. Phys. Soc. Jpn. **62**, 4449 (1993).
- ⁹ J. Richter, Phys. Rev. B **47**, 5794 (1993).
- ¹⁰ J. Richter, N. B. Ivanov, and K. Retzlaff, Europhys. Lett. **25**, 545 (1994).
- ¹¹ A. V. Dotsenko and O. P. Sushkov, Phys. Rev. B **50**, 13821 (1994).
- ¹² T. Einarsson and H. J. Schulz, Phys. Rev. B **51**, 6151 (1995).
- ¹³ M. E. Zhitomirsky and K. Ueda, Phys. Rev. B **54**, 9007 (1996).
- ¹⁴ M. S. L. du Croo de Jongh and P. J. H. Denteneer, Phys. Rev. B **55**, 2713 (1997).
- ¹⁵ R. F. Bishop, D. J. J. Farnell, and J. B. Parkinson, Phys. Rev. B **58**, 6394 (1998).
- ¹⁶ R. R. P. Singh, Z. Weihong, C. J. Hamer, and J. Oitmaa, Phys. Rev. B **60**, 7278 (1999).
- ¹⁷ L. Capriotti and S. Sorella, Phys. Rev. Lett. **84**, 3173 (2000).
- ¹⁸ L. Capriotti, Int. J. Mod. Phys. B **15**, 1799 (2001).
- ¹⁹ L. Siurakshina, D. Ihle, and R. Hayn, Phys. Rev. B **64**, 104406 (2001).
- ²⁰ O. P. Sushkov, J. Oitmaa, and Z. Weihong, Phys. Rev. B

- 63**, 104420 (2001).
- ²¹ L. Capriotti, F. Becca, A. Parola, and S. Sorella, Phys. Rev. Lett. **87**, 097201 (2001).
- ²² O. P. Sushkov, J. Oitmaa, and Z. Weihong, Phys. Rev. B **66**, 054401 (2002).
- ²³ L. Capriotti, F. Becca, A. Parola, and S. Sorella, Phys. Rev. B **67**, 212402 (2003).
- ²⁴ R. R. P. Singh, W. Zheng, J. Oitmaa, O. P. Sushkov, and C. J. Hamer, Phys. Rev. Lett. **91**, 017201 (2003).
- ²⁵ G. M. Zhang, H. Hu, and L. Yu, Phys. Rev. Lett. **91**, 067201 (2003).
- ²⁶ T. Roscilde, A. Feiguin, A. L. Chernyshev, S. Liu, and S. Haas, Phys. Rev. Lett. **93**, 017203 (2004).
- ²⁷ J. Sirker, Z. Weihong, O. P. Sushkov, and J. Oitmaa, Phys. Rev. B **73**, 184420 (2006).
- ²⁸ M. Mambrini, A. Läuchli, D. Poilblanc, and F. Mila, Phys. Rev. B **74**, 144422 (2006).
- ²⁹ D. Schmalfuß, R. Darradi, J. Richter, J. Schulenburg, and D. Ihle, Phys. Rev. Lett. **97**, 157201 (2006).
- ³⁰ F. Krüger and S. Scheidl, Europhys. Lett. **74**, 896 (2006).
- ³¹ T. Munehisa and Y. Munehisa J. Phys.: Condens. Matter **19**, 196202 (2007).
- ³² R. Melzi, P. Carretta, A. Lascialfari, M. Mambrini, M. Troyer, P. Millet, and F. Mila, Phys. Rev. Lett. **85**, 1318 (2000); P. Carretta, R. Melzi, N. Papinutto, and P. Millet, Phys. Rev. Lett. **88**, 047601 (2002); P. Carretta, N. Papinutto, C. B. Azzoni, M. C. Mozzati, E. Pavarini, S. Gonthier, and P. Millet, Phys. Rev. B **66**, 094420 (2002).
- ³³ H. Rosner, R. R. P. Singh, W. H. Zheng, J. Oitmaa, S.-L. Drechsler, and W. Pickett, Phys. Rev. Lett. **88**, 186405 (2002).
- ³⁴ A. Bombardi, J. Rodriguez-Carvajal, S. Di Matteo, F. de Bergevin, L. Paolasini, P. Carretta, P. Millet, and R. Caciuffo, Phys. Rev. Lett. **93**, 027202 (2004).
- ³⁵ R. Nath, A. A. Tsirlin, H. Rosner, and C. Geibel, Phys. Rev. B **78**, 064422 (2008).
- ³⁶ Y. Kamihara, T. Watanabe, M. Hirano, and H. Hosono, J. Am. Chem. Soc. **130**, 3296 (2008).
- ³⁷ T. Yildirim, Phys. Rev. Lett. **101**, 057010 (2008).
- ³⁸ Q. Si and E. Abrahams, Phys. Rev. Lett. **101**, 076401 (2008).
- ³⁹ F. Ma, Z.-Y. Lu, and T. Xiang, arXiv:0804.3370 (unpublished).
- ⁴⁰ T. Senthil, A. Vishwanath, L. Balents, S. Sachdev, and M. P. A. Fisher, Science **303**, 1490 (2004).
- ⁴¹ T. Senthil, L. Balents, S. Sachdev, A. Vishwanath, and M. P. A. Fisher, Phys. Rev. B **70**, 144407 (2004).
- ⁴² A. Gellé, A. M. Läuchli, B. Kumar, and F. Mila, Phys. Rev. B **77**, 014419 (2008).
- ⁴³ R. Kumar and B. Kumar, Phys. Rev. B **77**, 144413 (2008).
- ⁴⁴ A. W. Sandvik, Phys. Rev. Lett. **98**, 227202 (2007).
- ⁴⁵ A. B. Kuklov, M. Matsumoto, N. V. Prokof'ev, B. V. Svistunov, and M. Troyer, Phys. Rev. Lett. **101**, 050405 (2008).
- ⁴⁶ D. Yoshioka, G. Arakawa, I. Ichinose, and T. Matsui, Phys. Rev. B **70**, 174407 (2004).
- ⁴⁷ S. Wenzel, L. Bogacz, and W. Janke, Phys. Rev. Lett. **101**, 127202 (2008).
- ⁴⁸ F. Alet, G. Misguich, V. Pasquier, R. Moessner, and J. L. Jacobsen, Phys. Rev. Lett. **97**, 030403 (2006).
- ⁴⁹ S. Powell and J. T. Chalker, Phys. Rev. Lett. **101**, 155702 (2008).
- ⁵⁰ R. Schmidt, J. Schulenburg, J. Richter, and D. D. Betts, Phys. Rev. B **66**, 224406 (2002).
- ⁵¹ J. Oitmaa and W. Zheng, Phys. Rev. B **69**, 064416 (2004).
- ⁵² A. A. Nersesyan and A. M. Tsvetlik, Phys. Rev. B **67**, 024422 (2003).
- ⁵³ P. Sindzingre, Phys. Rev. B **69**, 094418 (2004).
- ⁵⁴ O. A. Starykh and L. Balents, Phys. Rev. Lett. **93**, 127202 (2004).
- ⁵⁵ S. Moukouri, J. Stat. Mech. (2006), P02002.
- ⁵⁶ R. F. Bishop, P. H. Y. Li, R. Darradi, and J. Richter, J. Phys.: Condens. Matter **20**, 255251 (2008).
- ⁵⁷ J. R. Viana and J. R. de Sousa, Phys. Rev. B **75**, 052403 (2007).
- ⁵⁸ R. F. Bishop, P. H. Y. Li, R. Darradi, J. Schulenburg, and J. Richter, Phys. Rev. B **78**, 054412 (2008).
- ⁵⁹ R. F. Bishop, P. H. Y. Li, R. Darradi, and J. Richter, Europhys. Lett. **83**, 47004 (2008).
- ⁶⁰ R. F. Bishop, P. H. Y. Li, R. Darradi, J. Richter, and C. E. Campbell, J. Phys.: Condens. Matter **20**, 415213 (2008).
- ⁶¹ F. Coester, Nucl. Phys. **7**, 421 (1958); F. Coester and H. Kümmel, *ibid.* **17**, 477 (1960).
- ⁶² R. F. Bishop, in *Microscopic Quantum Many-Body Theories and Their Applications*, Lecture Notes in Physics Vol. **510**, edited by J. Navarro and A. Polls, (Springer, Berlin, 1998), p. 1.
- ⁶³ M. Roger and J. H. Hetherington, Phys. Rev. B **41**, 200 (1990).
- ⁶⁴ R. F. Bishop, J. B. Parkinson, and Y. Xian, Phys. Rev. B **43**, 13782 (1991); Phys. Rev. B **44**, 9425 (1991).
- ⁶⁵ R. F. Bishop, R. G. Hale, and Y. Xian, Phys. Rev. Lett. **73**, 3157 (1994).
- ⁶⁶ C. Zeng, D. J. J. Farnell, and R. F. Bishop, J. Stat. Phys. **90**, 327 (1998).
- ⁶⁷ S. E. Krüger, J. Richter, J. Schulenburg, D. J. J. Farnell, and R. F. Bishop, Phys. Rev. B **61**, 14607 (2000).
- ⁶⁸ R. F. Bishop, D. J. J. Farnell, S. E. Krüger, J. B. Parkinson, and J. Richter, J. Phys.: Condens. Matter **12**, 6877 (2000).
- ⁶⁹ S. E. Krüger and J. Richter, Phys. Rev. B **64**, 024433 (2001).
- ⁷⁰ D. J. J. Farnell and R. F. Bishop, in *Quantum Magnetism*, Lecture Notes in Physics Vol. **645**, edited by U. Schollwöck, J. Richter, D. J. J. Farnell, and R. F. Bishop (Springer, Berlin, 2004), p. 307.
- ⁷¹ R. Darradi, J. Richter, and S. E. Krüger, J. Phys.: Condens. Matter **16**, 2681 (2004).
- ⁷² D. J. J. Farnell, J. Schulenburg, J. Richter, and K. A. Gerthof, Phys. Rev. B **72**, 172408 (2005).
- ⁷³ R. Darradi, J. Richter, and D. J. J. Farnell, Phys. Rev. B **72**, 104425 (2005).
- ⁷⁴ S. E. Krüger, R. Darradi, J. Richter, and D. J. J. Farnell, Phys. Rev. B **73**, 094404 (2006).
- ⁷⁵ R. Zinke, J. Schulenburg, and J. Richter, Eur. Phys. J. B **64**, 147 (2008).
- ⁷⁶ For the numerical calculation we use the program package The CRYSTALLOGRAPHIC CCM (D. J. J. Farnell and J. Schulenburg).
- ⁷⁷ A. V. Chubukov, S. Sachdev, and J. Ye, Phys. Rev. B **49**, 11919 (1994).
- ⁷⁸ R. Guida and J. Zinn-Justin, J. Phys. A **31**, 8103 (1998).
- ⁷⁹ B. I. Halperin and P. C. Hohenberg, Phys. Rev. **188**, 898 (1969).
- ⁸⁰ S. Chakravarty, B. I. Halperin, and D. R. Nelson, Phys. Rev. B **39**, 2344 (1989).
- ⁸¹ A. E. Trumper, L. O. Manuel, C. J. Gazza, and H. A. Cec-

catto, Phys. Rev. Lett. **78**, 2216 (1997); L. O. Manuel, A. E. Trumper, and H. A. Ceccatto, Phys. Rev. B **57**, 8348 (1998).

⁸² Note, however, that in Ref. 20 the response to a plaquette-

type modulation of bonds starting from a columnar dimerized state was calculated using series expansion.